

Control of Schottky Barrier Heights on High- K Gate Dielectrics for Future Complementary Metal-Oxide Semiconductor Devices

Koon-Yiu Tse and John Robertson

Engineering Department, Cambridge University, Cambridge CB2 1PZ, United Kingdom

(Received 5 March 2007; published 24 August 2007)

The calculated Schottky barrier heights of polar and nonpolar interfaces of many metals on HfO₂ high dielectric constant gate oxide have been found to vary strongly with the metal work function and also with oxide termination, with relatively little Fermi level pinning. This indicates that the choice of metal gate materials will not limit the continued scaling of metal-oxide semiconductor devices.

DOI: [10.1103/PhysRevLett.99.086805](https://doi.org/10.1103/PhysRevLett.99.086805)

PACS numbers: 73.30.+y, 73.40.Ns, 85.30.Tv

Metal—oxide interfaces are of critical importance for many applications such as catalysis, oxidation-resistant metals, and thermal barrier coatings. They have been studied by both models and *ab initio* calculations, particularly in terms of their interface energy and work of adhesion [1–6]. The continued scaling of Si field effect transistors (FET) has led to the replacement of the SiO₂ gate dielectric by a high dielectric constant (K) oxide such as HfO₂, and the doped polycrystalline Si gate electrode by a real metal [7,8]. The metal, which can be a compound or alloy, is chosen so that its work function, in contact with HfO₂, equals either the conduction band or valence band energy of Si, to create n -FET or p -FETs, respectively. However, some experimental data suggest that the barrier heights of metals on HfO₂ are partly “pinned” against changes in work function [9–11], casting doubt on whether such metals can easily be found. This would severely limit future device scaling. Recently, engineering solutions to the problem have been found [12–16]. Nevertheless, we clearly still need a deeper understanding of factors controlling Schottky barriers and “effective work functions” of metals on insulators [8,17,18].

The Schottky barrier height (SBH) is the energy difference between the metal Fermi level and the oxide conduction band. As the metal is varied, the barrier height ϕ_n can vary at a similar rate to the metal’s work function ϕ_M , viz $S = \partial\phi_n/\partial\phi_M \sim 1$. This is called the unpinned limit, as on SiO₂. At the opposite or “pinned” limit, the SBH hardly varies at all, with $S = \partial\phi_n/\partial\phi_M \sim 0$. HfO₂ is an oxide of medium band gap (6 eV) whose Schottky barrier behavior appears to lie midway between the pinned and unpinned limits, $S \sim 0.5$ [8]. The problem is that if $S = 0.5$, then we need two metals whose vacuum work functions differ by the band gap of silicon (1.1 eV) divided by S , or ~ 2.2 V [11]. This creates a problem, as low work function metals like La are very reactive, while high work function metals like Pt do not wet oxides and are difficult to etch.

To see if this problem is fundamental, we carried out detailed *ab initio* calculations of SBHs of many elemental metals at various lattice-matched interfaces on HfO₂, as a function of the oxygen chemical potential. We find that in

fact SBHs for a particular HfO₂ interface vary more strongly than $S = 0.5$ and are closer to the unpinned limit. In addition, SBHs vary significantly between different *interface stoichiometries* so that S is not the only factor, and accessible barrier heights easily span the needed range of 1.1 eV.

The existing simplified theory of Schottky barriers, using metal-induced gap states (MIGS) [18], ascribes SBH pinning to a finite density of MIGS pinning the SBH against changing metal Fermi energy. Its attraction is that it neglects specific interface geometry or chemistry. However, this is a significant omission. Once we do include real interface configurations, we must use lattice-matched interfaces. This is a severe limitation when trying to cover metals with a wide range of electronegativity. Cubic (fluorite) HfO₂ ($a = 5.12$ Å) has a good lattice match to fcc Ni ($a = 3.52$ Å) on (100), if the Ni lattice is rotated by 45°. However, many other metals match less well. We can create commensurate supercells with a forced lattice match, but we must then correct the interface energies for the strains of the individual components, as in [19]. Also, the Fermi energy of metals depends on strain, so this is also corrected for. We can enlarge the range of possible metals by considering metals in both their fcc and bcc phases, by noting that metal cohesive energy depends first on atomic volume and only second on structure [20].

There are three types of interfaces of polar compounds [21,22]: type 1 nonpolar interfaces like GaAs(100), type 2 consisting of nonpolar layer units like HfO₂ (111), and type 3 polar interfaces like GaAs(111) or HfO₂(100). Thus, HfO₂ has three interface stoichiometries: nonpolar, O-rich, and Hf-rich. For free surfaces, polar surfaces are unstable because of a finite electric field. However, polar surfaces are allowed next to metals because the metal creates an image charge to screen this field [23,24].

Figure 1 shows the O-rich and Hf-rich polar (100) interfaces of Ni on cubic HfO₂. We calculated various locations of Ni atoms above the oxide face and found that the most stable location was above two oxygens, giving a fourfold coordinated interface O site [25]. The most stable configuration of the Hf-terminated interface

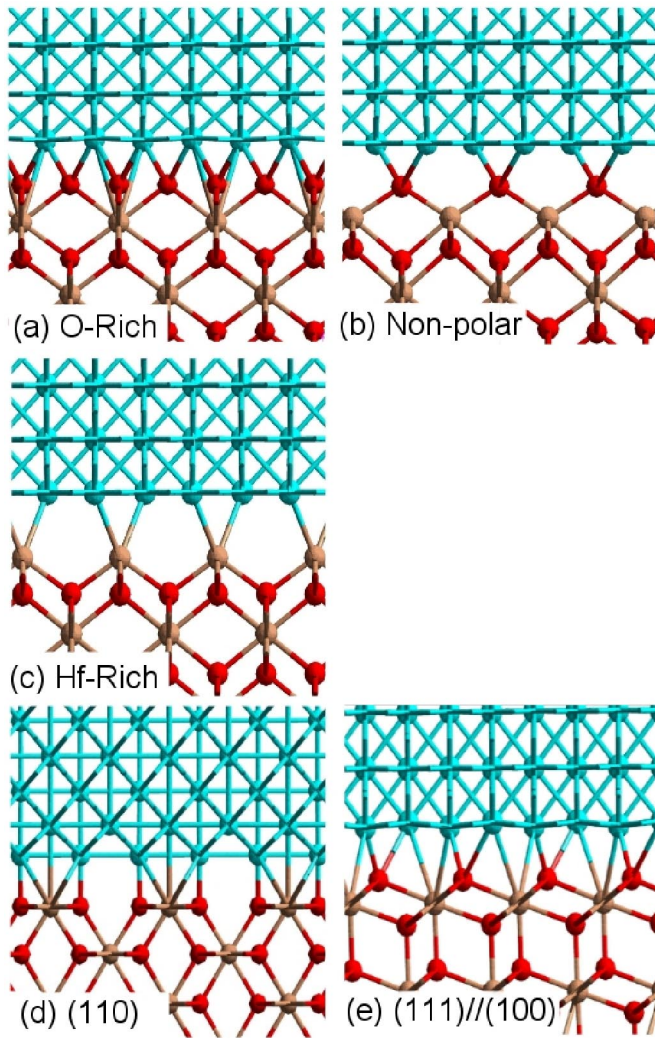


FIG. 1 (color online). Relaxed interface configurations of Ni:HfO₂. (a) O-rich, (b) nonpolar, (c) Hf-rich (100) interfaces, (d) nonpolar (110), and (e) nonpolar (111)HfO₂ on (100)Ni.

has the Hf above two Ni atoms, an overall 6-fold Hf coordination. Most other 3d transition metals also prefer these configurations. Our conclusions also hold for lower symmetry phases of HfO₂.

The (110) surface is the simplest nonpolar face of HfO₂. The 45° rotation still allows the formation of (110)HfO₂ || (110)Ni. The HfO₂(111) face is also nonpolar. However, as we cannot have 45° rotations about three axes, we cannot form (111)HfO₂ || (111)Ni. Carter [26] considered some commensurate (111) interfaces but with large cells. We constructed a small but strained HfO₂(111) || Ni(100) interface instead. A third possible nonpolar interface is to remove half the interface oxygens on O-rich (100). This gives three possible nonpolar HfO₂:Ni interfaces. Their relaxed structures are shown in Fig. 1(b). There are both Ni-O and Ni-Hf bonds at nonpolar interfaces.

We calculated the interface energies using the total energy pseudopotential code CASTEP [27] with a plane wave cutoff energy of 380 eV. The supercells have two

interfaces, 7 cells of metal, 5 units of HfO₂, and no vacuum. A k -space grid of $4 \times 4 \times 1$ to $8 \times 8 \times 1$ and $2 \times 4 \times 1$ to $4 \times 8 \times 1$ was used for the geometry relaxations of (001) and (011) faces, respectively [28]. The interface energy is derived from

$$E_{\text{int}} = \frac{E_{\text{Total}} - (nE_{\text{HfO}_2} + mE_{\text{Ni}} + l\mu_0)}{2q}$$

where 2 is the two interfaces per cell, q is the number of interface Ni atoms per face, n is the number of HfO₂ units per cell, E_{HfO_2} is the energy of a strained HfO₂ per formula unit, m is the number of metal atoms per cell, E_{Ni} is the energy of strained Ni per atom. l is the number of excess oxygen atoms not in a HfO₂ unit, and μ_0 is the chemical potential of oxygen as O₂.

The interfacial energy is plotted over the range of allowed oxygen chemical potentials in Fig. 2. At high chemical potentials, $\mu = 0$, the O-terminated interface is most stable. Its interfacial energy increases as μ decreases, until a nonpolar interface becomes most stable. Interestingly, nonpolar (100) is more stable than (110) or (111) when

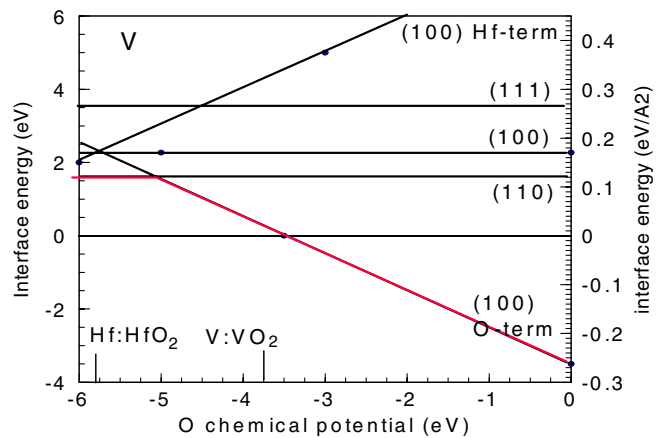
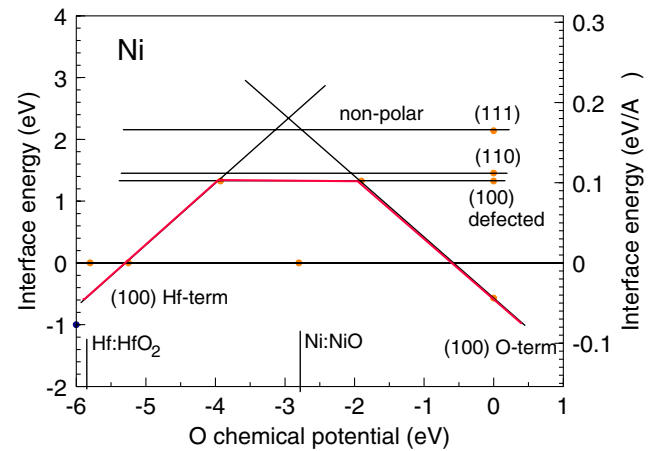


FIG. 2 (color online). Interface formation energies for Ni:HfO₂ and V:HfO₂ interfaces, as a function of oxygen chemical potential.

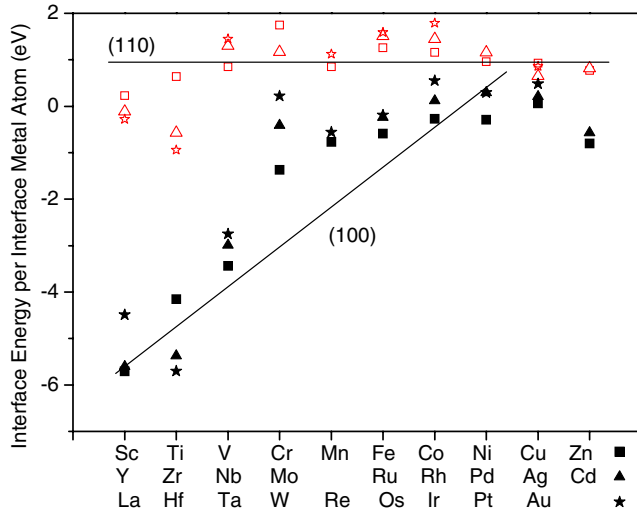


FIG. 3 (color online). Interface energies for (100) O-rich and (110) nonpolar metal: HfO_2 interfaces at $\mu = 0$, vs metal work functions.

expressed as J/m^2 rather than eV per surface Ni. This is because of the higher atomic density of (100). The (111) and (110) faces have similar density, and (110) is the more stable of these two. The nonpolar interfaces have no excess of O, so their formation energy is constant. At even lower μ values, the Hf-terminated (100) interface is most stable. We also indicate the μ_0 of the Ni:NiO reaction; it is above Hf: HfO_2 as Ni is more electropositive.

Figure 2 also shows an equivalent diagram for interfaces of a more electropositive metal V on HfO_2 . The O-terminated interface is most stable at high μ , the crossover to nonpolar occurs at much lower μ , and the Hf-terminated interface is never stable before the minimum μ .

Figure 3 shows the interface energies vs atomic number of the metal overlayer. We see that the interface energy of a polar O-terminated interface decreases as metal work function increases across the transition metal series. This is expected, as the interfacial M-O bond strength decreases as the metal WF increases. The same trend was found for metals on $\text{MgO}(111)$ [24]. Figure 3 also plots the formation energy of the nonpolar (110) interfaces against the metal WF, which show a flat trend.

The Schottky barrier heights were found by calculating the local density of states in the bulk oxide and metal layers, away from the interface, and taking the energy from oxide valence band maximum to the metal Fermi energy—the valence band offset (VBO). The alternative method of using electrostatic potentials and reference energies gives similar answers. Figure 4(a) plots VBO across the transition metal series and Fig. 4(b) plots VBO against metal work function [29]. A number of points are clear. First, the slope, S , of VBO vs WF is close to 1. Thus, the pinning factor S is rather unpinned, in realistic calculations, in contrast to the MIGS model. Second, the VBOs of (100) O-terminated interfaces are systematically ~ 0.8 eV

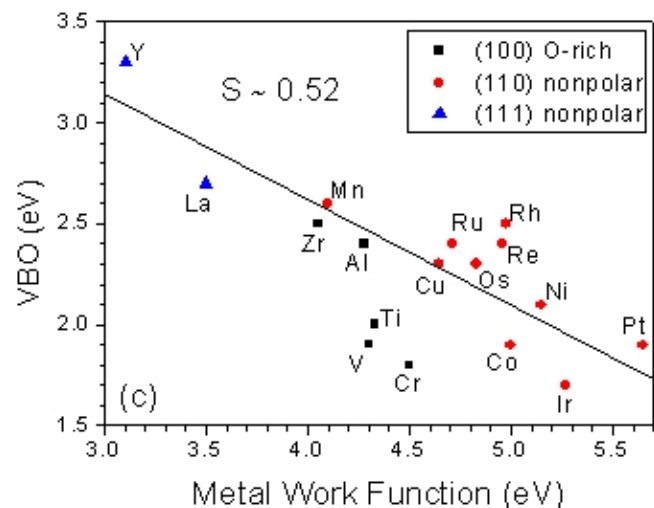
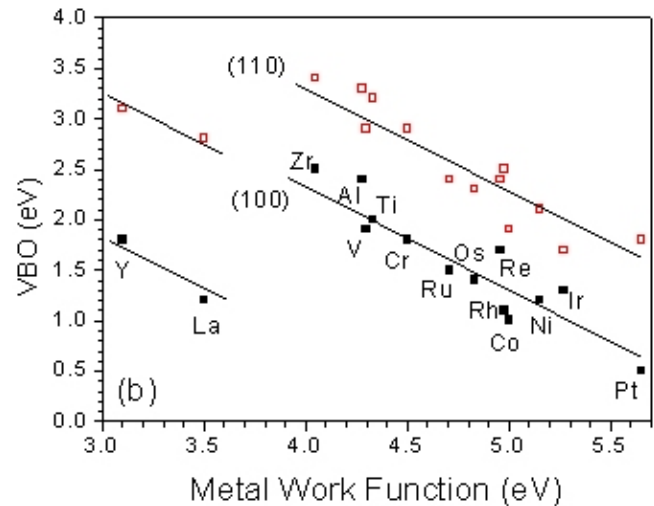
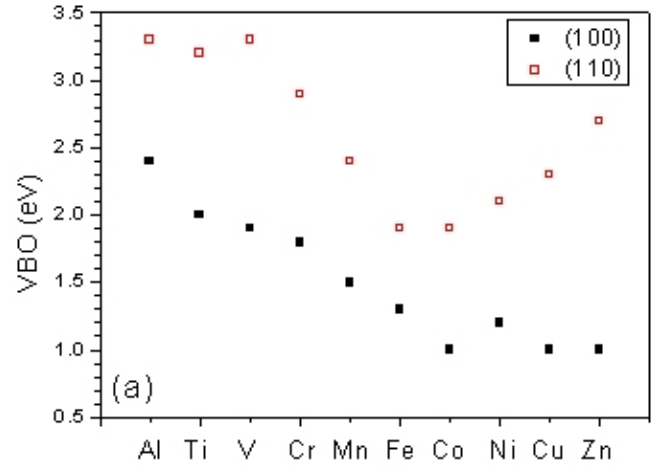


FIG. 4 (color online). Valence band offset of metals on (100) and (110) interfaces; (a) across the transition metal series, (b) vs metal work function, and (c) showing only stable interface at the O chemical potential of the $\text{M}:\text{MO}_n$ equilibrium.

lower than nonpolar (110) interfaces, a large offset. This means that there is an interface dipole, with the top metal layer systematically positive at the (100) O-rich interface. Including both these factors, the overall range of VBOs is large, large enough for engineering solutions to “Fermi level pinning.” Fourth, there is scatter in the trend lines in Fig. 4(b), as also found by Dong *et al.* [30]. Interestingly, there is a cleaner trend if VBO is plotted along the Period, Fig. 4(a), than against work function. Comparing to the experiment, the unpinned behavior found here is consistent with recent data [7] which likely exclude the extrinsic pinning effects.

It is more realistic to take VBOs at a certain O chemical potential, such as the M:MO equilibrium of the metal gate. In this case, Fig. 4(c) interestingly shows a smaller slope vs work function, $S \sim 0.52$. This is because the O-rich polar interfaces with smaller VBOs dominate for low WF metals and nonpolar interfaces for high WF metals.

The overall behavior found here indicates that the MIGS model may be somewhat too simplified model of the SB behavior of oxide—metal interfaces. The interface dipole does depend on interface termination, with much less pinning than in MIGS.

In conclusion, the calculated intrinsic Schottky barrier heights at metal/high- K oxide interfaces are unpinned, and a large range of SBHs are possible. These results are consistent with recent data [7]. This would therefore exclude intrinsic Schottky barrier effects as the cause of pinning. It suggests that pinning, when observed, is due to extrinsic effects such as oxygen vacancies [10,31,32]. This ought not to inhibit use of metal gates in semiconductor technology.

-
- [1] I. G. Batirev, A. Alavi, M. W. Finnis, and T. Deutsch, *Phys. Rev. Lett.* **82**, 1510 (1999).
 - [2] C. Verdozzi, D. R. Jennison, P. A. Schultz, and M. P. Sears, *Phys. Rev. Lett.* **82**, 799 (1999).
 - [3] A. Bogicevic and D. R. Jennison, *Phys. Rev. Lett.* **82**, 4050 (1999).
 - [4] X. G. Wang, A. Chaka, and M. Scheffler, *Phys. Rev. Lett.* **84**, 3650 (2000).
 - [5] S. A. Chambers, T. Droubay, Dr. R. Jennison, T. R. Mattson, *Science* **297**, 827 (2002).

- [6] M. W. Finnis, *J. Phys. Condens. Matter* **8**, 5811 (1996).
- [7] B. H. Lee *et al.*, *Mater. Today* **9**, 32 (2006).
- [8] J. Robertson, *Rep. Prog. Phys.* **69**, 327 (2006); *J. Vac. Sci. Technol. B* **18**, 1785 (2000).
- [9] J. K. Schaeffer *et al.*, in *Tech Digest* (Int. Electron Devices Meeting, 2004), p. 287.
- [10] E. Cartier *et al.*, *Tech Digest VLSI Technol Symp* (IEEE, New York, 2005), p. 15.
- [11] Y. C. Yeo, T. J. King, and C. Hu, *J. Appl. Phys.* **92**, 7266 (2002).
- [12] http://www.intel.com/technology/silicon/45nm_technology.htm.
- [13] S. Guha *et al.*, *Appl. Phys. Lett.* **90**, 092902 (2007).
- [14] H. N. AlShareef *et al.*, *Appl. Phys. Lett.* **89**, 232103 (2006).
- [15] X. P. Wang *et al.*, *IEEE Electron Device Lett.* **28**, 258 (2007).
- [16] H. N. Alshareef *et al.*, *Appl. Phys. Lett.* **88**, 112114 (2006).
- [17] W. Mönch, *Phys. Rev. Lett.* **58** 1260 (1987).
- [18] R. T. Tung, *Phys. Rev. Lett.* **84** 6078 (2000).
- [19] V. Fiorentini and G. Gulleri, *Phys. Rev. Lett.* **89**, 266101 (2002).
- [20] D. G. Pettifor, *Solid State Physics*, edited by Ehrenreich (Academic Press, Oxford, 1987) Vol. 40, p. 43.
- [21] P. W. Tasker, *J. Phys. C* **12**, 4977 (1979).
- [22] P. W. Peacock, and J. Robertson, *Phys. Rev. Lett.* **92** 057601 (2004).
- [23] A. M. Stoneham and P. W. Tasker, *J. Phys. C* **18** L543 (1985).
- [24] J. Goniakowski and C. Noguera, *Phys. Rev. B* **66** 085417 (2002); *Interface Sci.* **12**, 93 (2004).
- [25] J. L. Beltran, S. Gallego, J. Cerda, J. S. Moya, and M. C. Munoz, *Phys. Rev. B* **68**, 075401 (2003).
- [26] A. Christensen and E. A. Carter, *J. Chem. Phys.* **114**, 5816 (2001).
- [27] M. D. Segall, P. Lindan, M. J. Probert, C. J. Pickard, P. J. Hasnip, S. J. Clark, and M. C. Payne, *J. Phys. Condens. Matter* **14**, 2717 (2002).
- [28] Denser k point meshes were used to check convergence. The effects of strain on band offsets were allowed for as in ref. [19].
- [29] H. B. Michaelson, *J. Appl. Phys.* **48**, 4729 (1977).
- [30] Y. F. Dong, S. J. Wang, Y. P. Feng, and A. C. H. Huan, *Phys. Rev. B* **73**, 045302 (2006).
- [31] A. A. Demkov, *Phys. Rev. B* **74**, 085310 (2006).
- [32] Y. Akasaka *et al.*, *Jpn. J. Appl. Phys.* **45**, L1289 (2006).